Lagrangian Photochemical Modeling of Ozone Formation and Aerosol Evolution in Biomass Burning Plumes: Toward a Sub-grid Scale Parameterization

Matthew J. Alvarado*
Atmospheric and Environmental Research, Lexington, MA, USA

Robert J. Yokelson, Sheryl K. Akagi, and Ian R. Burling
University of Montana, Dept. of Chemistry, Missoula, MT, USA

Emily Fischer and G. R. McMeeking
Colorado State University, Dept. of Atmospheric Science, Fort Collins, CO, USA

K. Travis
Harvard University, School of Engineering and Applied Sciences, Cambridge, MA, USA

Jill S. Craven and John H. Seinfeld
California Institute of Technology, Division of Chemistry and Chemical Engineering, Pasadena, CA, USA

J. W. Taylor and H. Coe
University of Manchester, Centre for Atmospheric Science, Manchester, UK

S. P. Urbanski and C. E. Wold
USDA Forest Service Fire Sciences Lab, Missoula, MT, USA

D. R. Weise
USDA Forest Service Forest Fire Lab, Riverside, CA, USA

1. INTRODUCTION

Biomass burning is a major source of atmospheric pollution. Rapid, complex photochemistry can lead to significant increases in the concentrations of ozone in some smoke plumes after less than an hour of aging (e.g., Goode et al., 2000; Hobbs et al., 2003; Yokelson et al., 2009), while in other, generally boreal, plumes only small changes are observed on short time scales (e.g., Alvarado et al., 2010). Being able to simulate this rapid chemical evolution is a critical part of forecasting the impact of fires on urban and regional air quality.

The Aerosol Simulation Program (ASP) was developed to simulate the formation of ozone and secondary organic aerosol (SOA) within several African and North American plumes (Alvarado and Prinn, 2009). In this work, we discuss recent updates to the gas-phase chemistry and secondary organic aerosol (SOA) formation modules of ASP, and use this updated version (ASP v2.0) to simulate the chemical evolution of a

young biomass burning smoke plume sampled over California during the 2009 San Luis Obispo Biomass Burning campaign (Akagi et al., 2012). We then present our initial work in using ASP to develop a sub-grid scale parameterization of the near-source chemistry of biomass burning plumes for use in regional and global air quality models.

2. UPDATES TO THE AEROSOL SIMULATION PROGRAM (ASP)

2.1 Gas-phase Chemistry Updates

We have extensively updated the gas-phase chemistry within ASP. First, we updated all inorganic gas-phase chemistry within ASP to follow the latest IUPAC recommendations for kinetic rate constants. We also tested the JPL recommendations for these rate constants, but found that the differences between the recommendations generally made little difference to the model simulations, and as the IUPAC values were more in line with previous versions of ASP, these values were used.

Second, all gas-phase chemistry for organic compounds containing 4 carbons or less has been "unlumped," i.e. the chemistry for each individual

---

Corresponding author: Matthew J. Alvarado, Atmospheric and Environmental Research, 131 Hartwell Ave., Lexington, MA, 02421; e-mail: malvarad@aer.com

organic compound is explicitly resolved. This was done following the Leeds Master Chemical Mechanism (MCM) v3.2 (Saunders et al., 2003), available at http://mcm.leeds.ac.uk/MCM.

Third, we updated the chemical mechanism of isoprene within ASP to follow the Paulot et al. (2009a,b) isoprene scheme, as implemented in GEOS-Chem and including corrections based on more recent studies (e.g., Crounse et al., 2011, 2012).

Finally, the lumped chemistry for all other organic compounds in ASP has been updated to follow the Regional Atmospheric Chemistry Mechanism (RACM) v2 (Goliff et al., 2013).

2.2 SOA Formation Updates

We have updated the SOA formation module to follow the semi-empirical Volatility Basis Set (VBS) model of Robinson et al. (2007). Our implementation of this scheme followed the approach used by Ahmadov et al. (2012) to link the VBS scheme with the RACM chemical mechanism within WRF-Chem, with the exception that we use 9 VBS bins rather than only 4.

3. WILLIAMS FIRE

The Williams fire (34°41'45'' N, 120°12'23'' W) was sampled by the US Forest Service (USFS) Twin Otter aircraft from 10:50-15:20 LT on November 17, 2009. The fire burned approximately 81 hectares of scrub oak woodland understory and coastal sage scrub. Skies were clear all day and RH was low (11-26%) with variable winds (2-5 m/s). Full details on the measurements made are in Akagi et al. (2012). The plume showed significant secondary production of O_3 and peroxy acetyl nitrate (PAN), but the enhancement ratio of organic aerosol (OA) to CO_2 decreased slightly downwind.

4. ASP SIMULATION OF WILLIAMS FIRE

4.1 ASP Setup

As in Alvarado and Prinn (2009), we simulated the Williams fire smoke plume using ASP within a simple Lagrangian parcel model. The observed changes in CO mixing ratio were used to determine the best-fit model dilution rate, as well as upper and lower limits, as shown in Fig. 1.
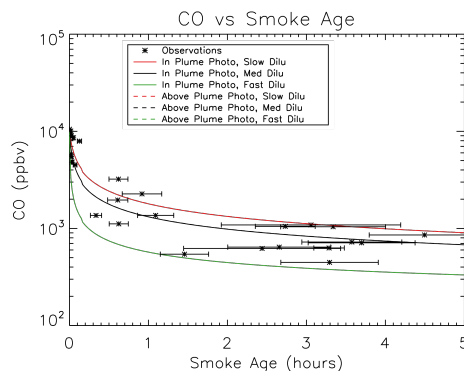

Fig. 1. CO mixing ratio (ppbv) versus smoke age. Red, black, and green are for the slow, best-fit (medium), and fast plume dilution rates. Asterisks are the measured mixing ratios, with the horizontal error bars showing the uncertainty in the estimated age.

Initial and background concentrations of trace gases and aerosols in the smoke were taken from observations of the Williams Fire (Akagi et al., 2012), where available. Emission ratios for other species were calculated using the literature reviews of Akagi et al. (2011) and Andreae and Merlet (2001). The volatility distribution for the primary organic aerosol (POA) was taken from the wood smoke study of Grieshop et al. (2009).
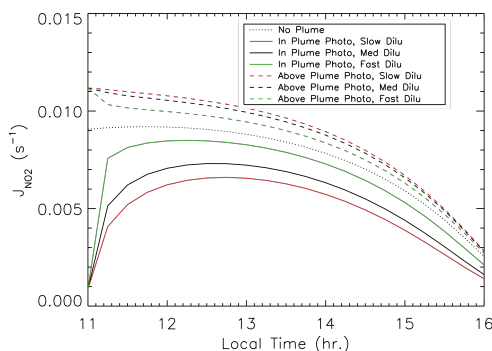

Fig. 2. NO_2 photolysis rates (s^{-1}) versus local time. Red, black, and green are for the slow, best-fit (medium), and fast plume dilution rates. Dashed lines are for above-plume photolysis rates, while solid lines are for the in-plume rates, as described in the text. The black dotted line is the clear-sky (no aerosol) photolysis rate.

Photolysis rates were calculated offline using TUV v5.0 (Madronich and Flocke, 1998). The smoke aerosols were assumed to dilute with time, and had an initial AOD at 330 nm of 8.0 and a single scattering albedo of 0.9. Photolysis rates were calculated within the plume (i.e., at 1.8 km within a plume extending from 1-2 km altitude) and just above the plume (i.e., at 2.1 km). This, combined with the three dilution rates, gave 6 estimates of photolysis rates versus time, which

2

are compared with the clear sky (no aerosol) case in Fig. 2.

4.2 Gas-Phase Results (Without SVOC Chemistry)

We first ran ASP assuming the uncharacterized semi-volatile organic compounds (SVOCs) emitted by the fire (following the volatility distribution of Grieshop et al., 2009) are unreactive. As shown in Figures 3 through 5, with this assumption ASP is able to simulate the change in O_3, NO_x, and peroxy acetyl nitrate (PAN) with time within the smoke plume.
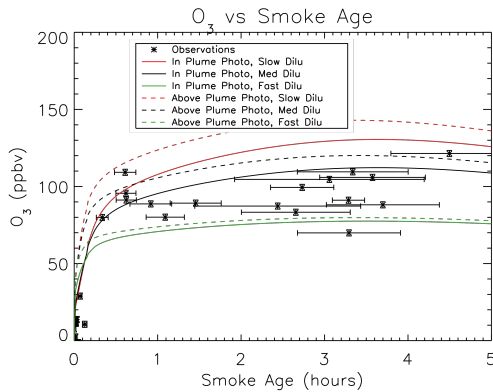

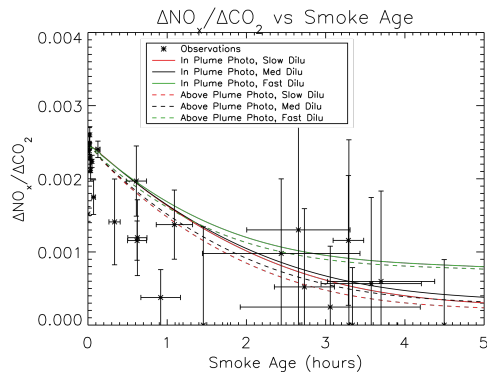Fig. 3. O_3 mixing ratio (ppbv) versus estimated smoke age.

Fig. 4. Enhancement ratio (mol/mol) of NO_x to CO_2 versus estimated smoke age ($\Delta NO_x = NO_{x,plume} - NO_{x,background}$).

ASP also does a good job of simulating the decay of C_2H_4 (not shown), suggesting that it is able to simulate the average OH concentration within the smoke plume. However, ASP underestimates the secondary production of aldehydes such as HCHO (see Fig. 6) and glycoaldehyde ($HCOCH_2OH$, not shown), as well

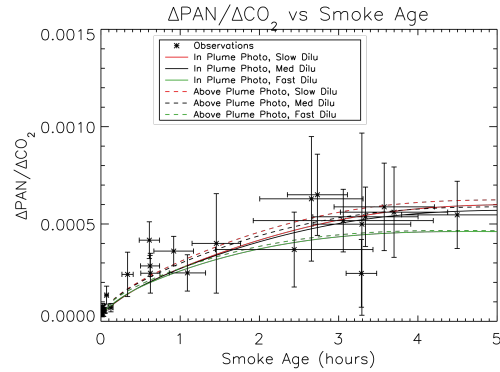as formic and acetic acid (not shown) within the Williams fire.

Fig. 5. Enhancement ratio (mol/mol) of PAN to CO_2 versus estimated smoke age.
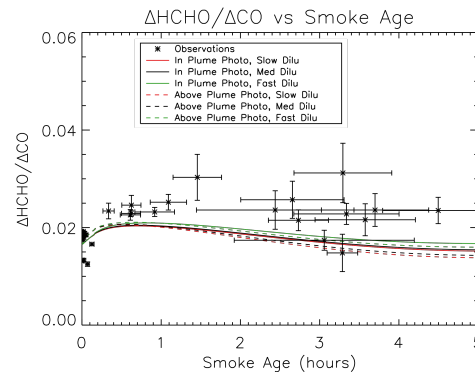

Fig. 6. Enhancement ratio (mol/mol) of HCHO to CO versus estimated smoke age.

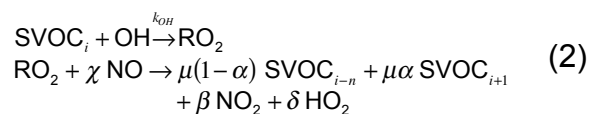## 4.3 Impact of SVOC Chemistry on SOA and O_3 formation

Above, we assumed that the SVOCs emitted by the fire were unreactive. In fact, like most organic compounds, SVOCs will react with OH. Most mechanisms for this chemistry (e.g., Robinson et al., 2007; Grieshop et al., 2009; Ahmadov et al., 2012) assume that the SVOCs react with OH to form a lower volatility SVOC, as in the equation:

$$\text{SVOC}_i + \text{OH} \xrightarrow{k_{OH}} \mu\text{SVOC}_{i-n} \quad (1)$$
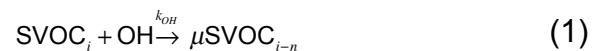
where μ is the relative mass gain from O addition, k_{OH} is the reaction rate with OH, and n is how many factors of 10 to lower the saturation mass concentration (C^*, see Robinson et al., 2007) of the product.

However, in reality after reaction with OH SVOCs produce peroxy radicals (RO_2), which can react with NO to form NO_2 and HO_2, thereby

3

regenerating OH and forming O_3. Equation 2 shows this more general chemical mechanism:

$$SVOC_i + OH \xrightarrow{k_{OH}} RO_2$$
$$RO_2 + \chi\,NO \rightarrow \mu(1-\alpha)\,SVOC_{i-n} + \mu\alpha\,SVOC_{i+1} \quad (2)$$
$$+ \beta\,NO_2 + \delta\,HO_2$$

where α is the fraction of RO_2 radicals that fragment. We can see that χ-β is the number of NO_x lost, 1-δ is the number of HO_x lost, and β+δ is the number of O_3 made per reaction. Table 1 shows the values for the parameters in the various SVOC mechanisms evaluated in this study.

Figure 7 shows the modeled OA enhancement ratios using the mechanisms listed in Table 1. We can see that the best match with observations is for k_{OH} = 10^{-11} cm^3/s, as in Ahmadov et al. (2012). However, even this case overestimates the amount of OA observed, and a fragmentation fraction (α) of 0.5 is needed to match the observed decay of the OA enhancement ratio.

Table 1. SVOC chemistry parameters in the mechanisms studied here.

Mechanism	k_{OH}x10^{11} (cm^3/s)	μ	n	α	χ	β	δ
Grieshop et al. (2009)	2.0	1.4	2	0	0	0	0
Robinson et al. (2007)	4.0	1.075	1	0	0	0	0
Ahmadov et al. (2012)	1.0	1.075	1	0	0	0	0
Ahmadov half frag.	1.0	1.075	1	.5	0	0	0
Ahmadov + NOx half frag.	1.0	1.075	1	.5	1	.65	.6

However, neglecting the chemistry of the peroxy radical, as in Eq. 1, leads to substantial underestimates of O_3, PAN, and OH. For example, using the Ahmadov et al. (2012) scheme reduces $\Delta O_3/\Delta CO_2$ to 4.7×10^{-3} at 4 to 4.5 hours, much lower than the observed value of $7.3(\pm1.6) \times 10^{-3}$ (Akagi et al., 2012). This is because including Eq. 1 in ASP leads to a loss of OH with no corresponding regeneration of HO_2 or conversion of NO to NO_2, reducing O_3 production.

Including the more realistic chemistry of Eq. 2 allows ASP to simultaneously simulate the observed changes in OA and O_3 by making reasonable assumptions about the chemistry of the SVOC "soup" emitted by the fire. For the Williams Fire, we find that the observed secondary O_3 formation is consistent with 1.25 O_3 formed per molecule of SVOC reacted, and that the best match with the observed decay of C_2H_4 is given by assuming that 60% of the OH reacted is

regenerated as HO_2 by the reaction of RO_2 with NO. However, this still underestimates the rate of decay of C_2H_4 within the smoke plume, due to an underestimate of the mean OH concentration (~3.2×10^6 molec/cm^3, versus the observed value of $5.3(\pm1.0) \times 10^6$ molec/cm^3).
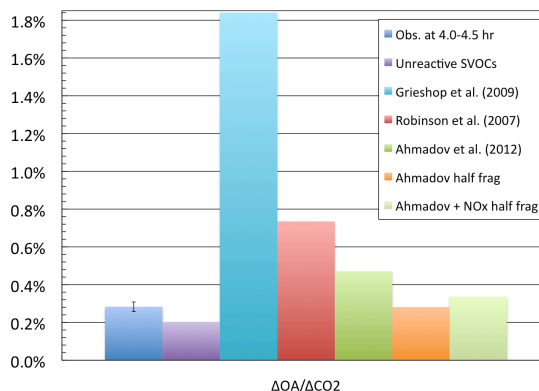

Fig. 7. Enhancement ratio (g/g) of organic aerosol (OA) to CO_2 after 4 to 4.5 hr of smoke aging.

5. TOWARD A SUB-GRID PARAMETERIZATION

We have begun to use the gas-phase results from ASP to simulate the sub-grid scale chemistry that takes place in smoke plumes within the GEOS-Chem model. Our initial plan is to use ASP to build a simple lookup table with three input variables: (1) fuel type, (2) temperature, and (3) beginning and ending solar zenith angles (SZA). The outputs will be enhancement ratios relative to CO (e.g., $\Delta O_3/\Delta CO$, $\Delta NO_x/\Delta CO$, $\Delta PAN/\Delta CO$) after 3 hours (although this timescale could be customized for finer scale models such as CMAQ), so that a simple multiplication by the biomass burning CO emissions within GEOS-Chem will give the "effective" emissions of these species after the sub-grid scale chemical processing has completed.

Tables 2 through 4 show some preliminary, example results from this work. Table 2 shows the enhancement ratios of O_3, NO_x, PAN, and inorganic nitrate ($HNO_{3(g)}$+$NO_{3(p)}$) for four different fuel types (savannah/grasslands, tropical forests, temperate forests, and boreal forests), all after 3 hours of aging with a constant SZA of 30° and constant temperature of 290 K. The base emission factors for each ecoregion are taken from Akagi et al. (2011) where available and from Andreae and Merlet (2001) otherwise. The initial concentrations in the plumes were normalized to give the same total mixing ratio of carbon in each plume – future work will explore the impact of environment and

fuel type on the initial plume concentrations. Tables 3 and 4 show the results for grassland smoke plumes for varying temperature and SZA, respectively.

Table 2. Enhancement ratios (mol/mol) after 3 h of aging at 290 K and SZA = 30°.

	Grassland /Savannah	Trop. Forest	Temp. Forest	Boreal Forest
$\Delta O_3/\Delta CO$	1.2×10^{-1}	1.1×10^{-1}	1.5×10^{-1}	3.7×10^{-2}
$\Delta NO_x/\Delta CO$	3.6×10^{-2}	5.6×10^{-3}	4.5×10^{-3}	3.2×10^{-4}
$\Delta PAN/\Delta CO$	7.6×10^{-3}	1.0×10^{-2}	1.2×10^{-2}	5.3×10^{-3}
$\Delta(Inorg. NO_3)/\Delta CO$	1.9×10^{-2}	1.2×10^{-2}	1.0×10^{-2}	3.2×10^{-3}

Table 3. Enhancement ratios (mol/mol) for grassland smoke after 3 h of aging at SZA of 10°.

	270 K	280 K	290 K	300 K
$\Delta O_3/\Delta CO$	1.2×10^{-1}	1.2×10^{-1}	1.4×10^{-1}	1.8×10^{-1}
$\Delta NO_x/\Delta CO$	3.7×10^{-2}	3.4×10^{-2}	3.4×10^{-2}	3.7×10^{-2}
$\Delta PAN/\Delta CO$	8.0×10^{-3}	8.6×10^{-3}	8.1×10^{-3}	5.2×10^{-4}
$\Delta(Inorg. NO_3)/\Delta CO$	2.0×10^{-2}	2.5×10^{-2}	1.9×10^{-2}	1.5×10^{-2}

Table 4. Enhancement ratios (mol/mol) for grassland smoke after 3 h of aging at 290 K.

	SZA = 0°	= 30°	= 60°	> 100°
$\Delta O_3/\Delta CO$	1.4×10^{-1}	1.2×10^{-1}	6.8×10^{-2}	-5.1×10^{-2}
$\Delta NO_x/\Delta CO$	3.4×10^{-2}	3.6×10^{-2}	4.3×10^{-2}	5.2×10^{-2}
$\Delta PAN/\Delta CO$	8.2×10^{-3}	7.6×10^{-3}	6.1×10^{-3}	2.0×10^{-4}
$\Delta(Inorg. NO_3)/\Delta CO$	1.9×10^{-2}	1.9×10^{-2}	1.8×10^{-2}	5.9×10^{-3}

The preliminary results generally follow expectations. Secondary O_3 production is higher for higher temperatures and lower SZAs, and boreal forests (which have a low NO_x/VOC emission ratio) have substantially less O_3 production than other fires under similar environmental conditions. However, temperate forests are predicted to have a higher O_3 formation than grasslands, which is inconsistent with field observations, and more work is needed to explain the discrepancy. The secondary production of PAN and inorganic nitrate also increases with decreasing SZA, but tends to peak at moderate temperatures (~280 K). At night (SZA > 100°), the smoke plume becomes a sink of O_3, as O_3 from the background air reacts with NO_x and alkenes within the smoke plume.

6. CONCLUSIONS

We have used the ASP model to simulate the near-source chemistry within the smoke plume from the Williams fire, as sampled by Akagi et al. (2012). We find that the assumptions made about the chemistry of the unidentified SVOCs emitted by the fire have a large impact on the simulated secondary formation of O_3, PAN, and OA within the plume. Specifically, neglecting the subsequent reaction of the peroxy radical (RO_2, formed by reaction of the SVOC with OH) with NO will lead to underestimates in the simulated O_3 and PAN concentrations.

We show that reasonable assumptions about the chemistry of the SVOCs can successfully simulate the observations. For the Williams fire, these assumptions are: (1) a reaction rate constant with OH of ~10^{-11} cm^3/ s; (2) a significant fraction (~50%) of the RO_2 + NO reaction results in fragmentation, rather than functionalization; (3) ~1.25 molecules of O_3 are formed for every molecule of SVOC that reacts; and (4) 60% of the OH that reacts with the SVOC is regenerated as HO_2 by the RO_2 + NO reaction. Similar studies of other young biomass burning plumes would allow us to see how the chemistry of the SVOC "soup" varies with fuel type, combustion efficiency, and other environmental parameters, providing an additional constraint on the reactivities of the unidentified SVOCs.

We have also presented preliminary results from our work to use the ASP model to develop a sub-grid parameterization of the chemistry within young smoke plumes for inclusion in larger chemical transport models. Our current approach focuses on determining how fuel type, temperature, and SZA impact the formation of O_3, inorganic nitrate, PAN and other organic nitrates within the smoke plume. Future work will evaluate the sensitivity of these formation rates to other environmental parameters (e.g., plume dilution rates) and incorporate these relationships into GEOS-Chem.

7. REFERENCES

Ahmadov, R., S. A. McKeen, A. L. Robinson, R. Bahreini, A. M. Middlebrook, J. A. de Gouw, J. Meagher, E.-Y. Hsie, E. Edgerton, S. Shaw, and M. Trainer, 2012: A volatility basis set model for summertime secondary organic aerosols over the eastern United States in 2006. *J. Geophys. Res.*, **117,** 2156-2202.

Akagi, S. K., R. J. Yokelson, C. Wiedinmyer, M. J. Alvarado, J. S. Reid, T. Karl, J. D. Crounse, and P. O. Wennberg, 2011: Emission factors for open and domestic biomass burning for

use in atmospheric models. *Atmos. Chem. Phys.*, **11,** 4039-4072.

Akagi, S. K., J. S. Craven, J. W. Taylor, G. R. McMeeking, R. J. Yokelson, I. R. Burling, S. P. Urbanski, C. E. Wold, J. H. Seinfeld, H. Coe, M. J. Alvarado, and D. R. Weise, 2012: Evolution of trace gases and particles emitted by a chaparral fire in California. *Atmos. Chem. Phys.*, **12,** 1397-1421.

Alvarado, M. J., and R. G. Prinn, 2009: Formation of Ozone and Growth of Aerosols in Young Smoke Plumes from Biomass Burning, Part 1: Lagrangian Parcel Studies. *J. Geophys. Res.*, **114,** D09306.

Alvarado, M. J., J. A. Logan, J. Mao, E. Apel, D. Riemer, D. Blake, R. C. Cohen, K.-E. Min, A. E. Perring, E. C. Browne, P. J. Wooldridge, G. S. Diskin, G. W. Sachse, H. Fuelberg, W. R. Sessions, D. L. Harrigan, G. Huey, J. Liao, A. Case-Hanks, J. L. Jimenez, M. J. Cubison, S. A. Vay, A. J. Weinheimer, D. J. Knapp, D. D. Montzka, F. M. Flocke, I. B. Pollack, P. O. Wennberg, A. Kurten, J. Crounse, J. M. St. Clair, A. Wisthaler, T. Mikoviny, R. M. Yantosca, C. C. Carouge, and P. Le Sager (2010), Nitrogen oxides and PAN in plumes from boreal fires during ARCTAS-B and their impact on ozone: an integrated analysis of aircraft and satellite observations, *Atmos. Chem. Phys.*, **10,** 9739-9760.

Andreae, M. O., and P. Merlet, 2001: Emission of trace gases and aerosols from biomass burning. *Global Biogeochem. Cycles*, **15,** 955-966.

Crounse, J. D., F. Paulot, H. G. Kjaergaard, and P. O. Wennberg, 2011: Peroxy radical isomerization in the oxidation of isoprene. *Phys. Chem. Chem. Phys.*, **13,** 13607-13613.

Crounse, J. D., H. C. Knap, K. B. Ørnsø, S. Jørgensen, F. Paulot, H. G. Kjaergaard, and P. O. Wennberg, 2012: Atmospheric Fate of Methacrolein. 1. Peroxy Radical Isomerization Following Addition of OH and O2. *J. Phys. Chem. A*, **116,** 5756-5762.

Goliff, W.S., W. R. Stockwell, and C. V. Lawson, 2013: The regional atmospheric chemistry mechanism, version 2. *Atmos. Environ.*, **68,** 174-185.

Goode, J. G., R. J. Yokelson, D. E. Ward, R. A. Susott, R. E. Babbitt, M. A. Davies, and W. M. Hao, 2000: Measurements of excess O3, CO2, CO, CH4, C2H4, C2H2, HCN, NO, NH3, HCOOH, CH3COOH, HCHO and CH3OH in 1997 Alaskan biomass burning plumes by airborne fourier transform infrared spectroscopy (AFTIR). *J. Geophys. Res.*, **105,** 22,147-22,166.

Grieshop, A. P., J. M. Logue, N. M. Donahue, and A. L. Robinson, 2009: Laboratory investigation of photochemical oxidation of organic aerosol from wood fires 1: measurement and simulation of organic aerosol evolution. *Atmos. Chem. Phys.*, **9,** 1263-1277.

Hobbs, P. V., P. Sinha, R. J. Yokelson, T. J. Christian, D. R. Blake, S. Gao, T. W. Kirchstetter, T. Novakov, and P. Pilewskie, 2003: Evolution of gases and particles from a savanna fire in South Africa. *J. Geophys. Res.*, **108,** 8485.

Madronich, S., and S. Flocke, 1998: The role of solar radiation in atmospheric chemistry. *Handbook of Environmental Chemistry*, P. Boule, Ed., Springer, 1-26.

Paulot, F., J. D. Crounse, H. G. Kjaergaard, J. H. Kroll, J. H. Seinfeld, and P. O. Wennberg, 2009a: Isoprene photooxidation: new insights into the production of acids and organic nitrates. *Atmos. Chem. Phys.*, **9**, 1479-1501.

Paulot, F., A. Kurten, J. M. St Clair, J. H. Seinfeld, and P. O. Wennberg, 2009b: Unexpected Epoxide Formation in the Gas-Phase Photooxidation of Isoprene. *Science*, **325**, 730-733.

Robinson, A. L., N. M. Donahue, M. K. Shrivastava, et al., 2007: Rethinking Organic Aerosols: Semivolatile Emissions and Photochemical Aging. *Science*, **315,** 1259-1262.

Saunders, S. M., M. E. Jenkin, R. G. Derwent, and M. J. Pilling, 2003: Protocol for the development of the Master Chemical Mechanism, MCM v3 (Part A): tropospheric degradation of non-aromatic volatile organic compounds. *Atmos. Chem. Phys.*, **3,** 161-180.

Yokelson, R. J., J. D. Crounse, P. F. DeCarlo, T. Karl, S. Urbanski, E. Atlas, T. Campos, Y. Shinozuka, V. Kapustin, A. D. Clarke, A. Weinheimer, D. J. Knapp, D. D. Montzka, J. Holloway, P. Weibring, F. Flocke, W. Zheng, D. Toohey, P. O. Wennberg, C. Wiedinmyer, L. Mauldin, A. Fried, D. Richter, J. Walega, J. L. Jimenez, K. Adachi, P. R. Buseck, S. R. Hall, and R. Shetter, 2009: Emissions from biomass burning in the Yucatan. *Atmos. Chem. Phys.*, **9,** 5785-5812.